Electronic structure of a stepped semiconductor surface: Density functional theory of Si(114)-(2×1)

R. D. Smardon,[1] G. P. Srivastava,[1] and S. J. Jenkins[2]
[1]*School of Physics, University of Exeter, Stocker Road, Exeter EX4 4QL, United Kingdom*
[2]*Department of Chemistry, University of Cambridge, Lensfield Road, Cambridge CB2 1EW, United Kingdom*
(Received 22 July 2003; revised manuscript received 12 November 2003; published 11 February 2004)

Ab initio density functional theory calculations, based on pseudopotentials and the plane-wave formalism, have been performed to investigate the equilibrium geometry, bonding, and electronic structure of the Si(114)-(2×1) surface, characterized by three prominent surface features (dimers, tetramers, and rebonded atoms). Several surface states are found in and around the bulk band gap. Mixing of the orbitals of the rebonded atoms with those of the dimers leads to a small band-gap surface.

DOI: 10.1103/PhysRevB.69.085303 PACS number(s): 73.21.−b, 68.35.Bs, 71.15.Mb

I. INTRODUCTION

High index semiconductor surfaces, such as Si(114), are technologically important and fundamentally interesting as many of these facets lie between the primary growth and cleavage planes. Such surfaces may display a variety of intricate and subtle surface properties that may profitably be exploited in future scientific and industrial applications. These features range from innate electronic properties through to surface deposition sites for layer growth. The morphology of high index surfaces is intimately correlated with the angle of orientation away from the densely-packed lower index planes. Large angular offsets produce grooved, sawtooth-like surfaces, whereas small angles lead to vicinal surfaces made up of (001)-terraces separated by occasional steps.[1] For surfaces with an orientation greater than 5° away from the low index (001) surface, as is the case with (114) surfaces, a large proportion of the resulting (001) terraces possess dimers orientated parallel to the step edges (*B*-type terraces). Stable Si(114) surfaces have been observed on etch pits formed on Si(001) and also cylindrical silicon samples.[2]

Between the primary growth and cleavage planes of Si [i.e., the (100) and (111) planes respectively], numerous different surfaces may be formed, with varying degrees of stability.[3] The Si(114) surface is canted from the (001) plane by 19.5° in the direction of the (111) plane, and comprises (001)-type terraces separated by double layer (DL) steps.[3] Indeed, the surfaces from (001) through to (117) generally display (001)-type terraces separated by steps, the dangling bond density and surface stress being lowered by the formation of rebonded atoms. A schematic representation of the (114) and (117) planes is given in Fig. 1. The surface energy is reduced further by the introduction of nonrebonded atoms at the step edge on the surfaces between (117) and (114) inclusive. This combination of rebonded and nonrebonded atoms leads to a highly stable surface geometry. Surfaces beyond (114) through to the (111) surface exhibit facets and sawtooth structures,[4] but Si(114) itself has a planar geometry that is thermodynamically resistant to faceting.

The Si(114) surface exhibits a (2×1) reconstruction, whose structure has been proposed by Erwin *et al.*[5] As shown in Fig. 2, the basic ingredients to this reconstruction are dimer formation and rebonding. A *B*-type dimer is formed along $[\bar{1}10]$ by the atoms labeled *A*. A tetramer is formed between atoms *C* and *D*, where atoms *C* form another *B*-type dimer (called a tetramer bridge) and the bond between atoms *C* and *D* (called tetramer arms) can be considered as *A*-type dimers. In addition, atoms labeled *B* are rebonded atoms. The formation of dimers is in close analogy with the (2×1) reconstruction of the (001) surface, whereby the *A*-type (*B*-type) dimers are perpendicular (parallel) to the step edge. The dimer formation reduces the number of unsaturated dangling bonds, thus lowering the surface energy. In addition, the rebonding decreases the surface energy further by saturation of extra dangling bonds at the step edge, following the proposal made by Chadi.[6] The surface thus exhibits a series of DL, *B*-type (001) terraces separated by rebonded *and* nonrebonded steps. This is schematically illustrated in Fig. 1. It is interesting to note that the density of dangling bonds on the Si(114)-(2×1) surface is almost identical to that of the common Si(001)-(2×1) surface at 0.064 and 0.068 db/Å^2 respectively, indicating the potential for Si(114)-(2×1) to form a stable surface. Figure 2 presents a schematic illustration of the atomic geometry of this surface.

To the best of our knowledge, there are no previously published results for the detailed electronic structure, density of states, or bonding characteristics of Si(114)-(2×1). This work presents a study of the surface geometry, electronic structure and density of states for this surface. In addition the bonding nature of the surface orbitals are provided and discussed.

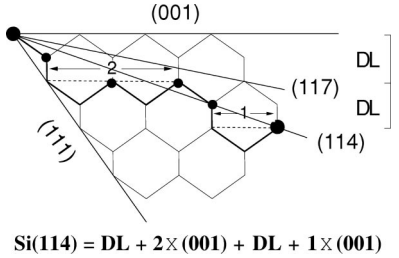

FIG. 1. A schematic representation of a few planes from (001) through to (111) for a tetrahedrally bonded crystalline material. Single and double width (001) terraces are indicated by the numbers 1 and 2, respectively. DL represents a double layer step.

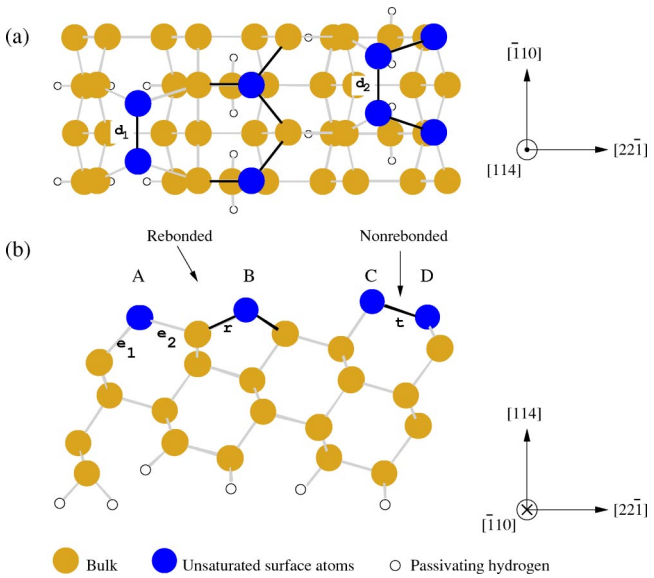

FIG. 2. A schematic representation of (a) a top and (b) a side view of the supercell used in our calculations modeling the Si(114)-(2×1) surface. *A*, dimer atoms; *B*, rebonded atoms; and *C* and *D* form a tetramer (*C*, dimer atoms and *D*, nonrebonded atoms). Other symbols are explained in the text.

II. METHODOLOGY

The results of all calculations presented in this paper are based on density functional theory within the local-density approximation (LDA). The parametrized Perdew and Zunger[7] form of the Ceperley-Alder[8] electron correlation scheme was used, and electron-ion interactions were described by the norm-conserving pseudopotentials of Troullier and Martins.[9] The relaxation of atomic and electronic degrees of freedom was achieved by solving the dynamic Kohn-Sham equations by a Car-Parrinello-like approach within a plane-wave basis set.[10,11]

The surface was modeled in a periodic slab geometry, the unit cells having the natural periodicity of the surface and an invoked artificial periodicity normal to the surface. Twelve layers of Si with an equivalent 12 layers of vacuum were modeled. The ''active'' surface was investigated while the opposite face of the slab was passivated with hydrogen. One layer of silicon atoms, adjacent to the passivating (hydrogen) atoms, was kept frozen in the bulk position and all other atoms were allowed to relax into their minimum-energy configuration. The surface geometry and electronic structure was obtained using a 12 Ryd kinetic energy cut-off. Test runs at 8, 10, 12 and 14 Ry cutoffs revealed that the structural and electronic parameters were well converged at the 12 Ry value. The theoretical bulk lattice constant of 5.42 Å was used in the surface calculations. Four special *k* points were used throughout for the sampling of the Brillouin zone.[12]

III. RESULTS

A. Atomic Structure

The structural relaxation of the Si(114)-(2×1) surface is characterized by three main features in accordance with the model proposed by Erwin *et al.*, as shown in Fig. 2. These are a dimer (*A*); rebonded atoms (*B*); and a tetramer (*C* and *D*). It is well documented[13] that the Si(001) surface undergoes a reconstruction and atomic relaxation whereby the dangling bonds become saturated or empty due to the formation of dimers. The same driving force is responsible for the formation of the dimer (*A*) features for the (114) surface. The rebonded atoms (*B*) arise from one of the two inequivalent DL step edges within the unit cell. Upon reconstruction each rebonded atom saturates one of its dangling bonds with a neighboring dangling bond. Finally, the tetramer arises from the combination of a dimer (*C*) and the nonrebonded step edge atoms (*D*). These three surface components, viz. the dimer, the rebonded atoms, and the tetramer, characterize the (114) surfaces of zinc blende as well as diamond-structure semiconductors.[14] All the surface features described above show some degree of buckling. Electronic charge transfer from an unsaturated dangling bond to an adjacent dangling bond leads to such tilting and thus gives rise to a local minimum-energy configuration.

Variations in the surface geometry were explored to investigate the minimum surface energy. In particular, multiple initial geometries with various degrees of surface buckling were considered (i.e, the geometries featured tilted dimers and tetramers, together with vertically asymmetric rebonded atoms). Upon relaxation, only two distinctly different local structural minima were located, with essentially equal energies, corresponding to a more or less ''flat tetramer'' structure and a rather more strongly ''buckled tetramer'' structure. These correspond to the two regimes of tetramer buckling described in the work of Erwin *et al.*[5] In each case, we find that the sense of the dimer tilt relative to the tetramer tilt has essentially no influence upon either the overall energetics or the local geometry of these features. This implies that the mechanism by which the surface saturates dangling bonds and releases strain is a predominantly local effect.

Structural parameters characterizing the relaxed surface are listed in Table I. The previous theoretical structural parameters calculated by Erwin *et al.*[5] are also listed for comparison. It can be seen that the dimer tilt, in both the present

TABLE I. Calculated values (in Å) of the key structural parameters shown in Fig. 2 for the Si(114)-(2×1) surface. Δ_D, Δ_{TD}, Δ_{NR}, and Δ_R are the vertical bucklings for the dimer, tetramer-dimer, nonrebonded, and rebonded atoms, respectively. The two values reported correspond to the low/high buckling models.

	This Work	Erwin *et al* (Ref. 5)
d_1	2.26	
Δ_D	0.23	0.17
d_2	2.34	
Δ_{TD}	0.10 / 0.25	0.00 / 0.30
t	2.22	
Δ_{NR}	0.00 / 0.08	0.00 / 0.15
r	2.47[a] and 2.43	
Δ_R	0.14 /0.40	0.18
e_1	2.41	
e_2	2.35	

[a]Higher rebonded atom

and the earlier study, is lower than that of the dimer tilt on the Si(001) surface. According to our calculation the dimer buckling is much smaller at 0.23 Å. Our calculations also suggest that the back bond linked to the ''upper dimer'' atom, length e_1, is 2% longer than the back bond linked to the ''lower dimer'' atom e_2. The inequivalence of the back bond length is a consequence of the dimer tilt and has also been identified for the Si(001)-(2×1) surface.[15]

The ''dimerlike'' bond of the tetramer, marked d_2 in Fig. 2, the so-called ''tetramer bridge,'' is rather longer than that of a common (001) dimer; some 4% larger in fact, due to the tension in the bonds marked ''t'' in Fig. 2. The t bonds, the so-called ''tetramer arms,'' are formed between each dimerlike tetramer atom and its adjacent ''nonrebonded'' tetramer atom. The rather short lengths of the tetramer arms indicate that they are strongly bonded. It appears that the tetramer arms are, in effect, similar to A-type (001) dimers, and that the tetramer bridge is a weakened B-type dimer.

The bonds ''r,'' formed by the rebonded atoms, are 5% longer than bulk Si-Si bonds. These extended bonds are caused by the highly strained nature of the rebonding near the step edge. Although the bond is exceedingly strained, throughout the calculations performed on this surface it showed no indication of breaking. The fact that various starting geometries of highly buckled rebonded atoms resulted in rather small forces and little change in overall energy indicates that this particular surface feature has a somewhat ''spongy'' character (i.e., a very flat contribution to the potential-energy hypersurface). The two buckling regimes of the tetramer and the spongy property of the rebonded atom together introduce the possibility of numerous distinct metastable forms of the Si(114)-(2×1) surface. The highly bucked rebonded atoms ($\Delta_R=0.40$ Å) and the highly buckled tetramer ($\Delta_{TD}=0.25$ Å) was found to be the minimum-energy configuration. Table I indicates the range of the tilting found for the rebonded atoms. The existence of a variety of metastable geometries for *both* the tetramer and the rebonded atoms was firmly established by considering a thicker slab and employing a higher kinetic-energy cutoff than that used in the previous theoretical calculations.[5]

Scanning tunnelling microscope (STM) images obtained by Erwin *et al.*[5] revealed two types of local reconstructions of (2×1) and $c(2\times2)$ symmetry. The $c(2\times2)$ symmetry differs from the (2×1) symmetry by the shifting of the surface features by half a primitive surface lattice vector in the $[\bar{1}10]$ direction. Erwin *et al.*[5] calculated the total energies of both reconstructions and found a difference at the level of only 1–2 meV/Å^2 between the two. This is too small an energy difference to favor one structure over another from their work. A Si(114)-$c(2\times2)$ structure was similarly found to be of a comparable energy with Si(114)-(2×1): a difference of ~1 meV/Å^2 in favor of the Si(114)-(2×1) reconstruction over the Si(114)-$c(2\times2)$ reconstruction (again no preferential structure can be deduced from this energy difference). Details of our results for the Si(114)-$c(2\times2)$ surface will be published elsewhere.

As is well established, there are two main driving processes for a nonpolar semiconductor surface to lower its energy:[16] ''structural reconstruction'' (i.e., the formation of the three surface features) and ''atomic relaxation'' (i.e., the buckling of these features along [114] as well as displacement of these with respect to the corresponding bulk positions). Our calculations suggest that the formation of the Si(114)-(2×1) surfaces with the above mentioned features results in a reduction of the surface energy by 6.9 eV per (2×1) surface unit cell, relative to the ideally terminated surface.

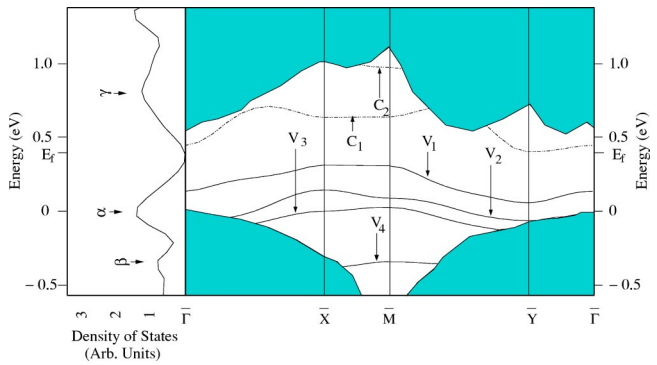

FIG. 3. Calculated band structure and density of states for the Si(114)-(2×1) surface. The surface bands are shown as heavy solid (occupied) and dashed (unoccupied) lines against the (2×1)-projected bulk structure for Si(114). The Fermi level is labeled E_F.

We have attempted to deduce the energy gain from each of the three surface reconstruction features as follows. Relative to the ideally bulk-terminated surface, the simple process of the dimer reconstruction formation (maintaining the dimer layer at the bulk-terminated height, i.e., the dimer height was constrained) was found to result in an energy gain of 1.40 eV. A similar consideration for the tetramer reconstruction resulted in an energy gain of 1.48 eV. Likewise, the energy gain from both rebonded atom formation was found to be 2.30 eV. A further gain of 1.7 eV results from the relaxation of the three reconstructed features. The relaxation energy is the difference between the sum of the individual reconstruction energies and the final structure total energy. A significant part of this comes from the relaxation of the center of mass of each of these features along the surface normal. A much smaller contribution comes from the relaxation around the center of mass (i.e., from buckling of the symmetrically reconstructed features). No extra energy is gained from the presence of nonrebonded atoms as they do not participate in any new bond formation. The combination of rebonded and nonrebonded steps is a compromise between surface stress and surface energy. Two rebonded steps would give an extremely stressed surface whereas two nonrebonded steps would give a high density of dangling bonds.

B. Electronic Structure

The electronic structure of Si(114)-(2×1) features a rich spectrum of surface bands within the silicon bulk band gap, as shown in Fig. 3. The slab used in the band calculation was the ''highly buckled tetramer'' and ''highly buckled rebonded atoms'' system. There are four occupied surface bands (of which one lies wholly above, and others partly above, the

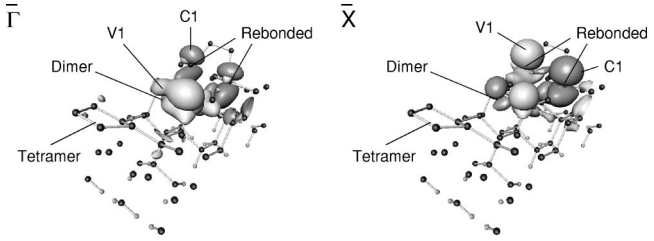

FIG. 4. Three-dimensional charge-density plots of the highest occupied and lowest unoccupied states at the Γ point and the X point for Si(114)-(2×1). The characteristic surface features are indicated. The isosurfaces are drawn at threshold charge densities of 2.0×10^{-3} $e/\text{Å}^3$.

bulk valence-band edge) and two unoccupied surface bands (one lying partly below the bulk conduction-band edge and the other wholly above). It can readily be seen that the highest occupied state at $\bar{X}$ (V_1) and the lowest unoccupied state at $\bar{Y}$ (C_1) almost overlap in energy. Although this gap lessens somewhat with decreasing tilt of the rebonded atoms (i.e. changing the tilt from 0.40 Å to 0.14 Å decreases the gap from 0.1 eV to 0.0 eV), the chemical potential nevertheless remains pinned between the V_1 maximum and the C_1 minimum. This demonstrates that Si(114)-(2×1) can range from a near zero band gap through to a small band-gap semiconductor of 0.1 eV in response to the metastable geometry of the rebonded atoms. We note, however, that a quasiparticle calculation (beyond the scope of the present work) would increase the band gap and may turn the surface into a somewhat larger band gap semiconductor.

The highest occupied state (V_1) is due to an elaborate mixture of the states from the dimer and the rebonded atoms. At the $\bar{\Gamma}$ point this state shows mainly π bonding between the dimer atoms (Fig. 4). At the $\bar{X}$ point, V_1 is mainly derived from the p_z orbital of the highest rebonded atom, with only a small contribution from the higher-lying dimer atom (Fig. 4). The V_1 state at the $\bar{M}$ point has the same characteristics as those at the $\bar{X}$ point, while the $\bar{Y}$ point is similar to $\bar{\Gamma}$, but with a little more contribution from the p_z orbital of the lower rebonded atom.

The lowest unoccupied state (C_1) is always predominantly localized on the rebonded atoms. Examining the $\bar{\Gamma}$ point again, C_1 is formed from in-phase p_z-like orbitals on both of the rebonded atoms. At the $\bar{X}$ point C_1 is localized predominantly on the lower rebonded atom, with a small out-of-phase p_z-like contribution from the lower-lying dimer atom. As with the V_1 state, the $\bar{M}$ point displays the same orbital structure as the $\bar{X}$ point and the partial density at the $\bar{Y}$ point is similar to that at the $\bar{\Gamma}$ point.

Clearly, folding the band structure of the unreconstructed (1×1) surface onto the (2×1) Brillouin zone ought to result in a degenerate pair of dispersionless states along the high-symmetry $\bar{X}$-$\bar{M}$ direction corresponding to linear combinations of the dangling bonds of the rebonded atoms. Splitting of these states, due both to Bragg scattering at the zone boundary and to the buckling of the rebonded atoms, would then generate the nondegenerate dispersionless pair of states V_1 and C_1 seen in the calculated band structure between $\bar{X}$ and $\bar{M}$. It is energetically more favorable to localize electrons in the dangling bond of the high-lying rebonded atom than in that of the low-lying one, as one might expect from simple electrostatic arguments. The well-separated orbital lobes of the C_1 state at the $\bar{\Gamma}$-$\bar{Y}$ axis provide a reference for the average energy of these dangling bonds, and the splitting of V_1 and C_1 at the $\bar{X}$-$\bar{M}$ axis is notably nearly symmetric about this level. The downward dispersion of the V_1 state in going from $\bar{X}$ to $\bar{\Gamma}$ (and from $\bar{M}$ to $\bar{Y}$) is likewise no mystery, corresponding to the onset of the in-phase π interactions which constitute the dimer bond.

Although we have focused upon what one might term the ''frontier'' surface states (i.e., the highest occupied and lowest unoccupied surface states), other characteristics of the surface band structure were also investigated (Fig. 5). Although these nonfrontier electronic bands have relatively little dispersion, these states nevertheless undergo complex changes in morphology with respect to changes in wave vector. In order to simplify matters, only surface states at special symmetry points will be discussed.

At the $\bar{M}$ point it is clear that six bands are surface localized, while at other points several of these are in resonance with the bulk. As seen in Figs. 5(a) and 5(b), the band V_2 at the $\bar{X}$ point is predominantly characterized by π bonding between the dimer atoms with a little p_z contribution from the higher rebonded atom. At the $\bar{M}$ point, however, it displays π bonding along each of the tetramer arms, both π orbitals being spatially well separated. The valence band labeled V_3 in Fig. 3 at the $\bar{X}$ point has similar characteristics to the band V_2 at the $\bar{M}$ point, as shown in Fig. 5(c). At the $\bar{M}$ point, however, the nature of the V_3 band is π bonding along the dimer, albeit with the majority of the charge being localized on the higher atom [Fig. 5(d)]. The fact that V_2 and V_3 more or less swap identities along the high-symmetry direction between $\bar{X}$ and $\bar{M}$ is indicative that there may be a degree of anticrossing between these bands. The band V_4 at the $\bar{M}$ point is a weak π bond along the tetramer bridge bond, biased somewhat towards the higher-lying side [Fig. 5(e)]. Finally the conduction band C_2, at both the $\bar{X}$ and the $\bar{M}$ points, is π antibonding along the higher-lying tetramer arm [Fig. 5(f)]. It is important to note here that all the surface bands have an underlying rebonded atom contribution. This contribution, although weak in comparison to the dominant features described above, plays a crucial role when it comes to sampling the bands in the form of STM images.

The calculated density of states for the Si(114)-(2×1) surface is also indicated in Fig. 3. Several dense peaks have been indicated, labeled α, β, and γ, close to the bulk band-gap region. The simulated as well as experimental STM results of Erwin *et al.* for the occupied surface states were investigated with a bias of -1.2 eV. Their STM image at this bias shows a large contribution from the rebonded atoms, with secondary features from the tetramer and the dimer atoms. From our density of states calculation a bias of

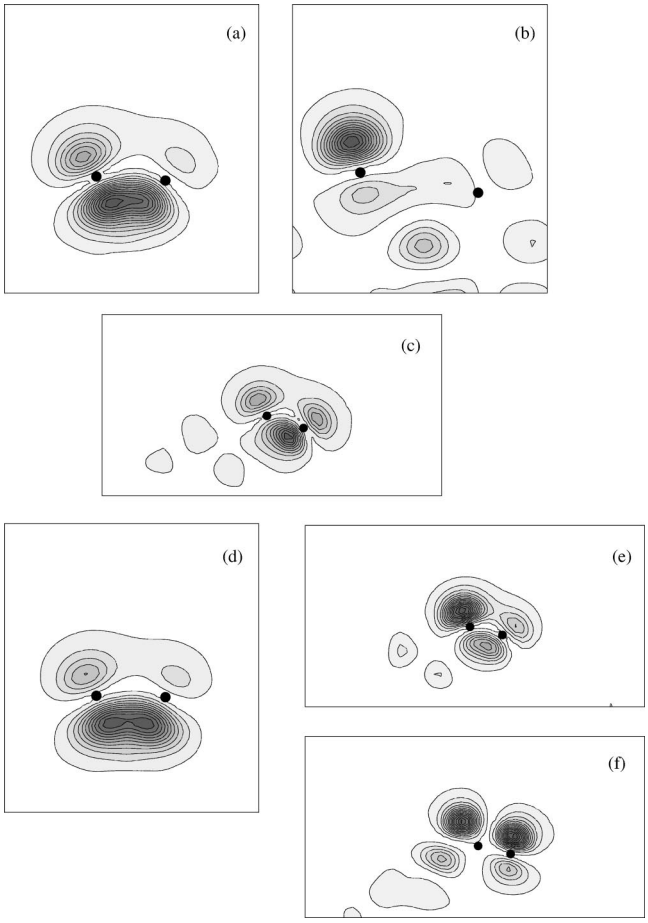

FIG. 5. Bonding characteristics of the Si(114)-(2×1) surface bands. The band $V_2(\bar{X})$ (meaning band V_2 at the $\bar{X}$ point) is contributed by (a) the π bonding of the dimer and (b) the p_z contribution from the higher rebonded atom. (c) shows the π bonding between one-half of the tetramer dimer and its adjacent nonrebonded atom for bands $V_2(\bar{M})$ and $V_3(\bar{X})$, with an identical plot for the other half of the tetramer. (d) represents the π bonding of the dimer for band $V_3(\bar{M})$. (e) depicts a π bond for the tetramer for $V_4(\bar{M})$, again with an equal plot for the other half. Finally, (f) signifies a weak π-bond for only one-half of the tetramer, the highest dimer, and its adjacent nonrebonded component, for the band C_2 at both the $\bar{X}$ and $\bar{M}$ points.

-1.2 eV would capture the peaks α and β. These peaks originate from the surface bands V_1, V_2, V_3, and V_4. As described before, although these four bands have charge densities associated with the tetramer and the dimer, the underlying rebonded contribution is dominant to these bands and thus in our density of states results. It can therefore be said that our density-of-states calculations are supportive of the experimental STM results. Such an agreement also exists between our density-of-states result and the STM results for the unoccupied states. A bias of 1.7 eV was used in the calculation by Erwin *et al.* and their STM plots show a dominant contribution from the rebonded atoms to the unoccupied bands with a smaller contribution from the tetramer. With the consideration of the shifting of our unoccupied bands (a compensation of around 0.6 eV for the shortfall of the unoccupied electronic bands of silicon within the LDA), the bias of 1.7 eV would capture the peak labeled γ. This peak is from the bands C_1 and C_2, which, as mentioned before, have charge associated largely with the rebonded atoms and the tetramer. With such an agreement between our density-of-states results and the STM work by Erwin *et al.*, we can be confident of the validity of our band-structure result.

Although the electronic structure of the Si(114)-$c(2\times2)$ surface has not been calculated, it is expected to exhibit properties similar to the Si(114)-(2×1) surface, in view of the apparent structural independence of the surface features. That is to say that the shifting of the rebonded atoms by half of a primitive surface lattice vector in the $[\bar{1}10]$ direction will not affect the structural parameters, and hence the features of the electronic band structure associated with the physical features of the atomic structure are expected to be largely unchanged.

IV. CONCLUSION

In conclusion, this paper presents results of *ab initio* calculations of the geometry, electronic structure, and orbital bonding nature of the reconstructed Si(114)-(2×1) surface. This high index surface appears to support a variety of metastable relaxation patterns, due to the elastic nature of the rebonded atoms and the tetramer. A rich array of surface states have been shown to result from a complex mixture of dangling bonds, and the surface LDA band gap ranges from near zero to around 0.1 eV dependent upon the particular metastable geometry adopted. The dispersion and character of the frontier surface states may be explained in terms of the dimer bond π interactions and the splitting of rebonded atom dangling bonds. The calculated density-of-states result is supportive of the STM work presented by Erwin *et al.*

ACKNOWLEDGMENTS

R.D.S. gratefully acknowledges financial support from the EPSRC(UK). S.J.J. is grateful to the Royal Society for financial support.

[1] B.S. Swartzentruber, N. Kitamura, M.G. Lagally, and M.B. Webb, Phys. Rev. B **47**, 13 432 (1993).
[2] T. Suzuki, Y. Tanishiro, H. Minoda, K. Yagi, and M. Suzuki, Surf. Sci. **298**, 473 (1993).
[3] A.A. Baski, S.C. Erwin, and L.J. Whitman, Surf. Sci. **392**, 69 (1997).
[4] S. Song and S.G.J. Mocherie, Phys. Rev. B **51**, 10 068 (1995).
[5] S.C. Erwin, A.A. Baski, and L.J. Whitman, Phys. Rev. Lett. **77**, 687 (1996).
[6] D.J. Chadi, Phys. Rev. Lett. **59**, 1691 (1987).
[7] J.P. Perdew and A. Zunger, Phys. Rev. B **23**, 5048 (1981).
[8] D.M. Ceperley and B.I. Alder, Phys. Rev. Lett. **45**, 566 (1980).

[9] N. Troullier and J.L. Martins, Phys. Rev. B **43**, 1993 (1991).
[10] G.P. Srivastava, J. Phys.: Condens. Matter **5**, 4695 (1993).
[11] M. Bockstedte, A. Kley, J. Neugebaer, and M. Scheffler, Comput. Phys. Commun. **107**, 187 (1997).
[12] R.A. Evarestov and V.P. Smirnov, Phys. Status Solidi B **119**, 9 (1983).
[13] S.J. Jenkins and G.P. Srivastava, J. Phys.: Condens. Matter **8**, 6641 (1996).
[14] J. Márquez, P. Kratzer, L. Geelhaar, K. Jacobi, and M. Scheffler, Phys. Rev. Lett. **86**, 115 (2001).
[15] S.C.A. Gay and G.P. Srivastava, Phys. Rev. B **60**, 1488 (1999).
[16] G.P. Srivastava, *Theoretical modelling of semiconductor surfaces* (World Scientific, Singapore, 1999).